Simultaneous super-resolution and blind deconvolution

2008 J. Phys.: Conf. Ser. 124 012048

(http://iopscience.iop.org/1742-6596/124/1/012048)

Journal of Physics: Conference Series **124** (2008) 012048 doi:10.1088/1742-6596/124/1/012048

Simultaneous super-resolution and blind deconvolution

F. Sroubek[1], G. Cristobal[2] and J. Flusser[1]

[1] Academy of Sciences, Pod vodárenskou věží 4 Prague, Czech Republic
[2] Instituto de Óptica (CSIC), Serrano 121, 28006 Madrid, Spain

Abstract. In many real applications, blur in input low-resolution images is a nuisance, which prevents traditional super-resolution methods from working correctly. This paper presents a unifying approach to the blind deconvolution and superresolution problem of multiple degraded low-resolution frames of the original scene. We introduce a method which assumes no prior information about the shape of degradation blurs and which is properly defined for any rational (fractional) resolution factor. The method minimizes a regularized energy function with respect to the high-resolution image and blurs, where regularization is carried out in both the image and blur domains. The blur regularization is based on a generalized multichannel blind deconvolution constraint. Experiments on real data illustrate robustness and utilization of the method.

1. Introduction

Imaging devices have limited achievable resolution due to many theoretical and practical restrictions. An original scene with a continuous intensity function $o(x, y)$ warps at the camera lens because of the scene motion and/or change of the camera position. In addition, several external effects such as atmospheric turbulence, camera lens, relative camera-scene motion, etc, can cause images to be blurred. We will call these effects *volatile blurs* to emphasize their unpredictable and transitory behavior, yet we will assume that we can model them as convolution with an unknown point spread function (PSF) $h(x, y)$. This is a reasonable assumption if the original scene is flat and perpendicular to the optical axis. Finally, the CCD discretizes the images and produces a digitized noisy image $g(i, j)$, which we refer to as a *low-resolution (LR) image*, since the spatial resolution is too low to capture all the details of the original scene. For one single observation $g(i, j)$ the problem of reconstructing $o(x, y)$ is heavily underdetermined and lacks stable solution. To partially overcome the equivocation of the problem, we can take K ($K > 1$) images of the original scene and face the so-called multichannel (multiframe) problem. The acquisition model then becomes

$$g_k(i, j) = D([h_k * W_k(o)](x, y)) + n_k(i, j)\,, \tag{1}$$

where $k = 1, \ldots, K$ is the acquisition index, $n_k(i, j)$ is additive noise and W_k denotes the geometric deformation (warping), in general different for each acquisition. $D(\cdot)$ is the *decimation operator* that models the function of CCD sensors. It consists of convolution with a *sensor PSF* followed by a *sampling operator*, which we define as multiplication by a sum of delta functions placed on a grid. The above model is the state of the art as it takes all possible degradations into account.

Superresolution (SR) is the process of combining a sequence of LR images in order to produce an image or sequence of higher resolution. It is unrealistic to assume that the superresolved image can recover the original scene $o(x, y)$ exactly. A reasonable goal of SR is a discrete version of $o(x, y)$, which has higher spatial resolution than the resolution of the LR images and which is free of the volatile blurs (deconvolved). In this paper, we will refer to this superresolved image as a *high resolution (HR) image* $f(i, j)$ and the ratio between the size of the sought HR image and input LR image will be called a *SR factor*. The standard SR approach consists of subpixel registration, overlaying the LR images on an HR grid, and interpolating the missing values. The subpixel shift between images thus constitutes an essential feature. We will demonstrate that considering volatile blurs in the model explicitly brings about a more general and robust technique, with the subpixel shift being a special case thereof.

The acquisition model in (1) embraces three distinct cases frequently encountered in the literature. First, removal of the geometric degradation W_k is a registration problem. Second, if the decimation operator D and the geometric transform W_k are not considered, we face a *multichannel* (or multiframe) *blind deconvolution* (MBD) problem. Third, if the volatile blur v_k is not considered or assumed known, and W_k is suppressed except to subpixel translations, we obtain a classical SR formulation. In practice, it is crucial to consider all three cases at once. We are then confronted with a problem of *blind superresolution* (BSR), the topic of this paper.

Proper registration techniques can suppress large and complex geometric distortions but usually a small between-image shift is still observable. There have been hundreds of methods proposed; see e.g. [1] for a survey. Here we will assume that registration parameters can be calculated by one of the methods, and if applied, the LR images are registered except to small translations.

Research on intrinsically MBD methods has begun fairly recently; refer to [2, 3, 4, 5, 6] for a survey and other references. The MBD methods can directly recover the blurring functions from the degraded images alone. We further developed the MBD theory in [7] by proposing a blind deconvolution method for images, which might be mutually shifted by unknown vectors. To make this brief survey complete, we should not forget to mention a very challenging problem of shift-variant blind deconvolution, that was considered in [8, 9].

A countless number of papers address the standard SR problem. A good survey can be found for example in [10, 11]. Maximum likelihood, maximum a posteriori (MAP), the set theoretic approach using projection on convex sets, and fast Fourier techniques can all provide a solution to the SR problem. Earlier approaches assumed that subpixel shifts are estimated by other means. More advanced techniques, such as in [12, 13, 14], include the shift estimation in the SR process. Other approaches focus on fast implementation [15], space-time SR [16], SR with complex image priors for joint image and segmentation estimation [17], or SR of compressed video [13]. Most of the SR techniques assume *a priori* known blurs. However, in many cases, such as camera motion, blurs can have wild shapes that are difficult to predict; see examples of real motion blurs in [18]. Authors in [19, 20, 21] proposed BSR that can handle parametric PSFs, i.e., PSFs modeled with one parameter. This restriction is unfortunately very limiting for most real applications. In [22] we extended our MBD method to BSR in an intuitive way but one can prove that this approach does not estimate PSFs accurately. The same intuitive approach was also proposed in [23]. To our knowledge, first attempts for theoretically correct BSR with an arbitrary PSF appeared in [24, 25]. The interesting idea proposed therein is to use so-called polyphase components. We will adopt the same idea here as well. Other preliminary results of the BSR problem with focus on fast calculation are given in [26], where the authors propose a modification of the Richardson-Lucy algorithm.

Current MBD techniques require no or very little prior information about the blurs, they are sufficiently robust to noise and provide satisfying results in most real applications. However, they can hardly cope with the decimation operator, which violates the standard convolution

model. On the contrary, state-of-the-art SR techniques achieve remarkable results of resolution enhancement in the case of no blur. They accurately estimate the subpixel shift between images but lack any apparatus for calculating the blurs.

Recently in [27], we proposed a unifying method that simultaneously estimates the volatile blurs and HR image. The only prior knowledge required are estimates of the blur size and level of noise in the LR images, which renders it a truly BSR method. The key idea was to determine subpixel shifts by calculating volatile blurs. As the volatile blurs are estimated in the HR scale, positions of their centroids correspond to sub-pixel shifts. Therefore by estimating blurs we automatically estimate shifts with sub-pixel accuracy, which is essential for good performance of SR. We show that the blurs in the HR scale can be recovered from the LR images up to small ambiguity, which is a generalization of results obtained for blur estimation in the MBD case and which we have proposed earlier in [22, 27]. This complex SR problem was solved by minimizing a regularized energy function, where the regularization was carried out in both the image and blur domains. The image regularization is based on variational integrals, and a consequent anisotropic diffusion with good edge-preserving capabilities. The blur regularization term is based on our generalized result of blur estimation in the SR case. To tackle the minimization task, we used an alternating minimization approach consisting of two simple linear equations.

In this work, we extend the BSR method by incorporating registration parameters. In Section 2 we present the regularized energy functional and derive the regularization terms. The alternating minimization scheme and parameter estimation is given in Section 3. Finally, Section 4 illustrates applicability of the proposed method to real situations.

2. Blind Superresolution

In order to solve the BSR problem, i.e, determine the HR image f and volatile PSFs h_k, we adopt an approach of minimizing a regularized energy function. This way the method will be less vulnerable to noise and better posed. The energy, using vector-matrix notation, consists of three terms and takes the form

$$E(\mathbf{f},\mathbf{h}) = \sum_{k=1}^{K} \|\mathbf{D}_k\mathbf{H}_k\mathbf{f} - \mathbf{g}_k\|^2 + Q(\mathbf{f}) + R(\mathbf{h})\,, \tag{2}$$

where $\mathbf{h} = [\mathbf{h}_1^T, \ldots, \mathbf{h}_K^T]^T$, $\mathbf{D}_k$ represents the discrete case of $\mathbf{D}$ that includes H_k (the warping) and $\mathbf{W}_k$ denotes a matrix that represents convolution with $\mathbf{h}_K$. The first term measures the fidelity to the data and emanates from our acquisition model (1). The remaining two are regularization terms that attract the minimum of E to an admissible set of solutions. The form of E very much resembles the energy proposed in [7] for MBD. Indeed, this should not come as a surprise since MBD and SR are related problems in our formulation. Regularization $Q(\mathbf{f})$ is a smoothing term of the form

$$Q(\mathbf{f}) = \alpha\mathbf{f}^T\mathbf{L}\mathbf{f}\,, \tag{3}$$

where $\mathbf{L}$ is a high-pass filter and α is a positive regularization parameter. A common strategy is to use convolution with the Laplacian for $\mathbf{L}$, which in the continuous case, corresponds to $Q(f) = \int |\nabla f|^2$. Recently, variational integrals $Q(f) = \int \phi(|\nabla f|)$ were proposed, where ϕ is a strictly convex, nondecreasing function that grows at most linearly. Examples of $\phi(s)$ are s (total variation), $\sqrt{1+s^2}-1$ (hypersurface minimal function), $\log(\cosh(s))$, or nonconvex functions, such as $\log(1+s^2)$, $s^2/(1+s^2)$ and $\arctan(s^2)$ (Mumford-Shah functional). The advantage of the variational approach is that while in smooth areas it has the same isotropic behavior as the Laplacian, it also preserves edges in images. The disadvantage is that it is highly nonlinear and to overcome this difficulty, one must use, e.g., half-quadratic algorithm [32]. For the purpose of our discussion it suffices to state that after discretization we arrive again at (3), where this

time $\mathbf{L}$ is a positive semidefinite block tridiagonal matrix constructed of values depending on the gradient of f. The rationale behind the choice of $Q(f)$ is to constrain the local spatial behavior of images; it resembles a Markov Random Field. Some global constraints may be more desirable but are difficult (often impossible) to define, since we develop a general method that should work with any class of images. Our PSF regularization term $R(\mathbf{h})$ consists of two terms. The first one is the same smoothing term as for images but applied to blurs, which is a typical prior that penalizes jagged blurs that are rare in real situations. The second term is a consistency term that binds the different volatile PSFs to prevent them from moving freely and unlike the fidelity term (the first term in (2)) it is based solely on the observed LR images. It takes the form of $\|\mathcal{N}\mathbf{h}\|^2$ (see [27]). The complete PSF regularization is then give by

$$R(\mathbf{h}) = \beta \mathbf{h}^T \mathbf{L} \mathbf{h} + \gamma \|\mathcal{N}\mathbf{h}\|^2 \,, \tag{4}$$

where β and γ are positive regularization parameters that give different weights to the terms.

3. Alternating minimization

The complete energy function reads

$$E(\mathbf{f}, \mathbf{h}) = \sum_{k=1}^{K} \|\mathbf{D}_k \mathbf{H}_k \mathbf{f} - \mathbf{g}_k\|^2 + \alpha \mathbf{f}^T \mathbf{L} \mathbf{f} + \mathbf{h}^T (\beta \mathbf{L} + \gamma \mathcal{N}^T \mathcal{N}) \mathbf{h} \,. \tag{5}$$

To find a minimizer, we perform alternating minimizations (AM) of E over $\mathbf{f}$ and $\mathbf{h}$. The advantage of this scheme lies in its simplicity. Each term of (5) is quadratic and therefore convex (but not necessarily strictly convex) and the derivatives w.r.t. $\mathbf{f}$ and $\mathbf{h}$ are easy to calculate. This AM approach is a variation on the steepest-descent algorithm. The search space is a concatenation of the blur subspace and the image subspace. The algorithm first descends in the image subspace and after reaching the minimum, i.e., $\nabla_{\mathbf{f}} E = 0$, it advances in the blur subspace in the direction $\nabla_{\mathbf{h}} E$ orthogonal to the previous one, and this scheme repeats. In conclusion, starting with some initial $\mathbf{h}^0$ the two iterative steps are:

step 1.

$$\begin{aligned} \mathbf{f}^m &= \arg\min_{\mathbf{f}} E(\mathbf{f}, \mathbf{h}^m) \\ &\Leftrightarrow \text{solve for } \mathbf{f} \\ &\quad (\sum_{k=1}^{K} \mathbf{H}_k^T \mathbf{D}_k^T \mathbf{D}_k \mathbf{H}_k + \alpha \mathbf{L}) \mathbf{f} = \sum_{k=1}^{K} \mathbf{H}_k^T \mathbf{D}_k^T \mathbf{g}_k \,, \end{aligned} \tag{6}$$

step 2.

$$\begin{aligned} \mathbf{h}^{m+1} &= \arg\min_{\mathbf{h}} E(\mathbf{f}^m, \mathbf{h}) \\ &\Leftrightarrow \text{solve for } \mathbf{h} \\ &\quad ([\mathbf{I}_K \otimes \mathbf{F}^T \mathbf{D}_k^T \mathbf{D}_k \mathbf{F}] + \gamma \mathcal{N}^T \mathcal{N} + \beta \mathbf{L}) \mathbf{h} \\ &\quad = [\mathbf{I}_K \otimes \mathbf{F}^T \mathbf{D}_k^T] \mathbf{g} \,, \end{aligned} \tag{7}$$

where $\mathbf{F}$ represents the convolution with f, $\mathbf{g} := [\mathbf{g}_1^T, \ldots, \mathbf{g}_K^T]^T$, $\otimes$ is the Kronecker product, $\mathbf{I}_K$ the identity matrix of size k and m is the iteration step. Note that both steps consist of simple linear equations.

Because it is a function of both variables f and h, the energy E is not convex due to coupling of variables via convolution in the first term of (5). Therefore, it is not guaranteed that the

BSR algorithm reaches the global minimum, instead, one may get trapped in local minima. In our experience, convergence properties improve significantly if we add feasible regions for the HR image and PSFs specified as lower and upper bound constraints. To solve step 1, we use the method of conjugate gradients (function *cgs* in Matlab) and then adjust the solution $\mathbf{f}^m$ to contain values in the admissible range, typically, the range of values of $\mathbf{g}$. It is common to assume that PSF is positive ($h_k \geq 0$) and that it preserves image brightness. We can therefore write the lower and upper bounds constraints for PSFs as $0 \leq h_k \leq 1$. In order to enforce the bound in step 2, we solve (7) as a constrained minimization problem (function *fmincon* in Matlab) rather than using the projection as in step 1. Constrained minimization problems are more computationally demanding but we can afford it in this case since the size of $\mathbf{h}$ is much smaller than the size of $\mathbf{f}$.

Parameters α, β and γ depend on the level of noise. If noise increases, α and β should increase, and γ should decrease. One can prove that α and β are proportional to σ_n^2, which is the noise variance, assuming Gaussian white noise. Estimation techniques, such as cross-validation [19] or expectation maximization [34], can be used to determine the correct weights. However, we did not want to increase complexity of the problem any further and thus we set the values in experiments manually according to our visual assessment. If the iterative algorithm begins to amplify noise, we have underestimated the noise level. On the other hand, if the algorithm begins to segment the image, we have overestimated the noise level.

4. Experiments

The following experiments with the proposed BSR method aim to first compare perfomance with other techniques and second demonstrate its applicability to real scenarios with misregistered input images.

4.1. Real data

The first experiment demonstrates a task of license plate recognition. With an Olympus C5050Z digital camera we took eight photos, registered them with cross correlation and cropped each to 156x56 pixels. Three of the LR images enlarged with zero-order interpolation is shown in Fig. 1a. The described BSR method returned a well reconstructed HR image (Fig. 1b), which is comparable to the ground truth acquired with the optical zoom (Fig. 1d). A SR-only method provides lower performance (see Fig. 1c). In our case the SR-only method is a maximum a posteriori (MAP) formulation of the SR problem proposed, e.g., in [12, 13]. This method uses a MAP framework for the joint estimation of image registration parameters and the HR image, assuming only the sensor blur and no volatile blurs. For an image prior, we used edge preserving Huber Markov Random Fields (MRF) [35]. A potential pitfall that we have to take into consideration is a feasible range of SR factors. As the SR factor increases we need to take more LR images and the stability of BSR decreases. Hence we limit the SR factor between 1 and 2.5 in most practical applications.

The second group of three experiments demonstrate the advantage of using the decimation operators $\mathbf{D}_k$'s with registration instead of running BSR on registered LR images. Three video sequences were taken from the Farsiu & Milanfar SR dataset[15] [1]. Fig. 2(a) shows one frame out of ten corresponding to the "Disk" sequence. In a previous publication [31], we estimated registration parameters and compared two approaches. First, we applied BSR on registered images. Second, we used the registration parameters to construct $\mathbf{D}_k$'s and applied BSR on the original unregistered images. Some small details are better reconstructed in the second approach, which indicates that using the registration parameters directly in BSR is preferable. Fig. 2(b) shows the result of the second approach. Similarly, Fig. 2(c) shows one frame out of

[1] http://www.soe.ucsc.edu/∼milanfar/DataSets/

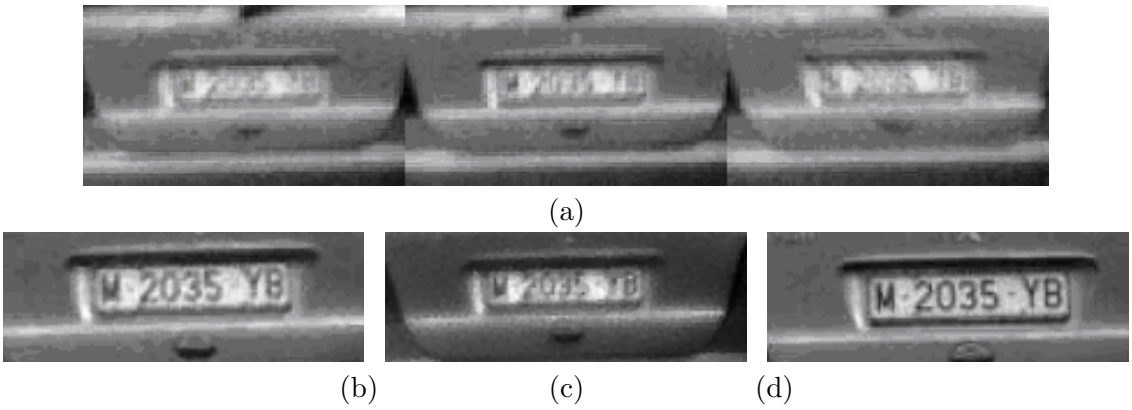

(a) (b) (c) (d)

Figure 1. (a) Shown are three LR frames. (b) The BSR result. (c) The SR result. (d) Optical zoom reference.

ten corresponding to the "Text" sequence and Fig. 2(d) the BSR result. Finally, Fig. 2(e) shows one frame out of ten corresponding to the "Car" sequence and Fig. 2(f) the BSR result. In all the cases the SR factor used was 2.

(a) (b) (c) (d) (e) (f)

Figure 2. Superresolution with registration. (a) Shown is one "Disk" LR frame from the Farsiu & Milanfar dataset. (b) BSR result. (c) Shown is one "Text" LR frame from the same dataset. (d) BSR result. (e) Shown is one "Car" LR frame from the same dataset. (f) BSR result.

5. Conclusions

This paper presented a SR method which proved to be meaningful for cases when an insufficient number of input LR images is available to perform SR with only integer factors, such as two or three. To achieve truly robust methodology applicable in real situations, we adopted the regularized energy minimization approach, which we solve by an alternating-minimization scheme. The fundamental improvement on previously proposed SR methods is the notion of estimating PSFs in the HR scale, which indirectly aligns LR images with subpixel accuracy. Using registration parameters inside the algorithm instead of registering input images gives better results and paves the way for including methods of making registration parameters more accurate during reconstruction of the HR image [31, 36]

Acknowledgments

This work has been partially supported by the projects TEC 2004-00834, TEC2005-24739-E, TEC2005-24046-E, PI040765, 2004CZ0009 CSIC-Academy of Sciences of the Czech Republic,

No. 202/05/0242 of the Grant Agency of the Czech Republic and No. 1M0572 (Research Center DAR) of the Czech Ministry of Education.

References

[1] Zitová, B. and Flusser, J. (2003) Image registration methods: A survey. *Image and Vision Computing*, **21**, 977–1000.
[2] Harikumar, G. and Bresler, Y. (1999) Perfect blind restoration of images blurred by multiple filters: Theory and efficient algorithms. *IEEE Trans. Image Processing*, **8**, 202–219.
[3] Giannakis, G. and Heath, R. (2000) Blind identification of multichannel FIR blurs and perfect image restoration. *IEEE Trans. Image Processing*, **9**, 1877–1896.
[4] Pai, H.-T. and Bovik, A. (2001) On eigenstructure-based direct multichannel blind image restoration. *IEEE Trans. Image Processing*, **10**, 1434–1446.
[5] Panci, G., Campisi, P., Colonnese, S., and Scarano, G. (2003) Multichannel blind image deconvolution using the bussgang algorithm: Spatial and multiresolution approaches. *IEEE Trans. Image Processing*, **12**, 1324–1337.
[6] Šroubek, F. and Flusser, J. (2003) Multichannel blind iterative image restoration. *IEEE Trans. Image Processing*, **12**, 1094–1106.
[7] Šroubek, F. and Flusser, J. (2005) Multichannel blind deconvolution of spatially misaligned images. *IEEE Trans. Image Processing*, **14**, 874–883.
[8] You, Y.-L. and Kaveh, M. (1999) Blind image restoration by anisotropic regularization. *IEEE Trans. Image Processing*, **8**, 396–407.
[9] Rajagopalan, A. and Chaudhuri, S. (1999) An MRF model-based approach to simultaneous recovery of depth and restoration from defocused images. *IEEE Trans. Pattern Analysis and Machine Intelligence*, **21**, 577–589.
[10] Park, S., Park, M., and Kang, M. (2003) Super-resolution image reconstruction: A technical overview. *IEEE Signal Proc. Magazine*, **20**, 21–36.
[11] Farsui, S., Robinson, D., Elad, M., and Milanfar, P. (2004) Advances and challenges in super-resolution. *Int. J. Imag. Syst. Technol.*, **14**, 47–57.
[12] Hardie, R., Barnard, K., and Armstrong, E. (1997) Joint map registration and high-resolution image estimation using a sequence of undersampled images. *IEEE Trans. Image Processing*, **6**, 1621–1633.
[13] Segall, C., Katsaggelos, A., Molina, R., and Mateos, J. (2004) Bayesian resolution enhancement of compressed video. *IEEE Trans. Image Processing*, **13**, 898–911.
[14] Woods, N., Galatsanos, N., and Katsaggelos, A. (2006) Stochastic methods for joint registration, restoration, and interpolation of multiple undersampled images. *IEEE Trans. Image Processing*, **15**, 201–213.
[15] Farsiu, S., Robinson, M., Elad, M., and Milanfar, P. (2004) Fast and robust multiframe super resolution. *IEEE Trans. Image Processing*, **13**, 1327–1344.
[16] Shechtman, E., Caspi, Y., and Irani, M. (2005) Space-time super-resolution. *IEEE Trans. Pattern Analysis and Machine Intelligence*, **27**, 531–545.
[17] Humblot, F. and Muhammad-Djafari, A. (2006) Super-resolution using hidden markov model and bayesian detection estimation framework. *EURASIP Journal on Applied Signal Processing*, **2006**, 36971.
[18] Ben-Ezra, M. and Nayer, S. (2004) Notion-based motion deblurring. *IEEE Trans. Pattern Analysis and Machine Intelligence*, **26**, 689–698.
[19] Nguyen, N., Milanfar, P., and Golub, G. (2001) Efficient generalized cross-validation with applications to parametric image restoration and resolution enhancement. *IEEE Trans. Image Processing*, **10**, 1299–1308.
[20] Woods, N., Galatsanos, N., and Katsaggelos, A. (2003) EM-based simultaneous registration, restoration, and interpolation of super-resolved images. *Proceeding of ICIP*, Barcelona, September, pp. 303–306. IEEE Computer Society.
[21] Rajan, D. and Chaudhuri, S. (2003) Simultaneous estimation of super-resolved scene and depth map from low resolution defocused observations. *IEEE Trans. Pattern Analysis and Machine Intelligence*, **25**, 1102–1117.
[22] Šroubek, F. and Flusser, J. (2006) Resolution enhancement via probabilistic deconvolution of multiple degraded images. *Pattern Recognition Letters*, **27**, 287–293.
[23] Chen, Y., Luo, Y., and Hu, D. (2005) A general approach to blind image super-resolution using a PDE framework. *Proceedings of SPIE*, Beijing, July, pp. 1819–1830. SPIE.
[24] Wirawan, Duhamel, P., and Maitre, H. (1999) Multi-channel high resolution blind image restoration. *Proceedings of ICASSP*, Phoenix, AR, March, pp. 3229–3232. IEEE Computer Society.
[25] Yagle, A. (2003) Blind superresolution from undersampled blurred measurements. *Proceedings of SPIE*, Bellingham, December, pp. 299–309. SPIE.

[26] Biggs, D., C.L.Wang, Holmes, T., and Khodjakov, A. (2004) Subpixel deconvolution of 3D optical microscope imagery. *Proceedings of SPIE*, Denver, CO, October, pp. 369–380. SPIE.
[27] Šroubek, F., Cristóbal, G., and Flusser, J. (2007) A unified approach to superresolution and multichannel blind deconvolution. *IEEE Trans. Image Processing*, **16**, 2322–2332.
[28] Lin, Z. and Shum, H.-Y. (2004) Fundamental limits of reconstruction-based superresolution algorithms under local translation. *IEEE Trans. Pattern Analysis and Machine Intelligence*, **26**, 83–97.
[29] Pelletier, S. and Cooperstock, J. (2007) Fast super-resolution for rational magnification factors. *Proceedings of ICIP*, San Antonio, TX, September, pp. 65–68. IEEE Computer Society.
[30] Šroubek, F., Flusser, J., and Cristóbal, G. (2007) Multiframe blind deconvolution coupled with frame registration and resolution enhancement. In Campisi, P. and Egiazarian, K. (eds.), *Blind Image Deconvolution: Theory and Applications*. CRC Press, FL.
[31] Šroubek, F., Flusser, J. and Cristóbal, G. (2007) Superresolution and blind deconvolution for rational factors. *The Computer Journal*, in press.
[32] Aubert, G. and Kornprobst, P. (2002) *Mathematical Problems in Image Processing*. Springer Verlag, New York.
[33] Tschumperlé, D. (2002) PDE's Based Regularization of Multivalued Images and Applications. PhD thesis University of Nice-Sophia Antipolis.
[34] Molina, R., Vega, M., Abad, J., and Katsaggelos, A. (2003) Parameter estimation in Bayesian high-resolution image reconstruction with multisensors. *IEEE Trans. Image Processing*, **12**, 1655–1667.
[35] Capel, D. (2004) *Image Mosaicing and Super-Resolution*. Springer, New York.
[36] Chung, J., Haber, E., and Nagy, J. (2006) Numerical methods for coupled super-resolution. *Inverse Problems*, **22**, 1261–1272.